

# RSC Advances

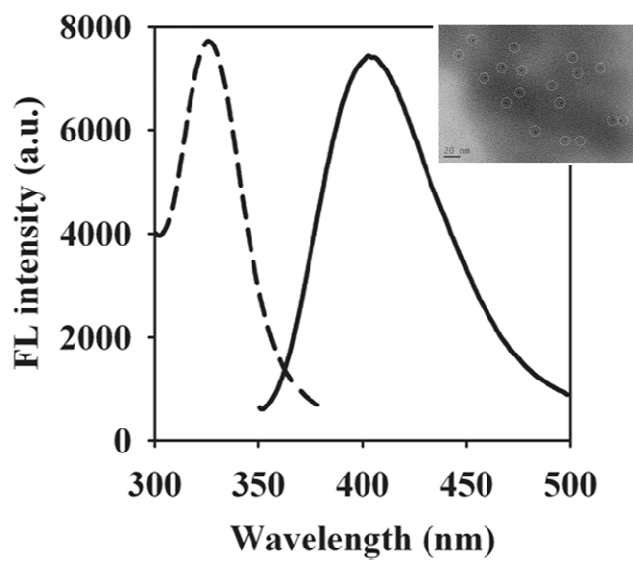


This is an *Accepted Manuscript*, which has been through the Royal Society of Chemistry peer review process and has been accepted for publication.

*Accepted Manuscripts* are published online shortly after acceptance, before technical editing, formatting and proof reading. Using this free service, authors can make their results available to the community, in citable form, before we publish the edited article. This *Accepted Manuscript* will be replaced by the edited, formatted and paginated article as soon as this is available.

You can find more information about *Accepted Manuscripts* in the [Information for Authors](#).

Please note that technical editing may introduce minor changes to the text and/or graphics, which may alter content. The journal's standard [Terms & Conditions](#) and the [Ethical guidelines](#) still apply. In no event shall the Royal Society of Chemistry be held responsible for any errors or omissions in this *Accepted Manuscript* or any consequences arising from the use of any information it contains.



**Novel fabrication of highly fluorescent Pt nanoclusters and their  
applications in hypochlorite assay**

Xiaodong Xia, Yu Zhang, Jianxiu Wang\*

College of Chemistry and Chemical Engineering, Central South University, Changsha,

Hunan, P. R. China 410083

---

\* Corresponding author. E-mail: [jxiuwang@csu.edu.cn](mailto:jxiuwang@csu.edu.cn)

**Abstract**

A simple and efficient method for the fabrication of highly fluorescent platinum nanoclusters (Pt NCs) has been reported in which bovine serum albumin (BSA) serves as a scaffold and  $\text{NaBH}_4$  as a reductant. The BSA-stabilized Pt NCs possess uniform morphology with sub-nanometer sizes. In comparison with other reports for the synthesis of the Pt NCs, our method involves less time and very mild experimental conditions. Hypochlorite sensing has been achieved via examining the fluorescence intensity of the Pt NCs and the fluorescence quenching involves the oxidation of the Pt NCs. The proof-of-concept experiment demonstrates that Pt NCs could serve as a viable alternative for selective hypochlorite assay.

**Keywords:** Pt NCs; facile synthesis; fluorescence quenching; hypochlorite assay

## 1. Introduction

Water-soluble noble metal nanoclusters (Cu,<sup>1</sup> Ag,<sup>2</sup> Au,<sup>3</sup> and Pt NCs<sup>4</sup>) emit strong fluorescence, thus holding great potential for applications in chemical/biological sensing and cellular imaging. Typically, these NCs consist of several or tens of metal atoms with size close to the Fermi wavelength of an electron and their emission properties depend on the size quantization,<sup>5</sup> surface ligands,<sup>6</sup> and even the microenvironment around the NCs.<sup>7</sup> The metal NCs have proven to be advantageous in that they are soluble, biocompatible, photostable, and possess high brightness.<sup>1,3,7</sup>

Unlike other metal NCs, such as Cu,<sup>1</sup> Ag,<sup>2</sup> and Au NCs,<sup>3</sup> the fluorescent Pt NCs are rather difficult to synthesize. For example, yellow-emitting Pt NCs have been constructed via etching Pt nanoparticles by glutathione and the most intense fluorescence was obtained at 65 °C after 6 days.<sup>8</sup> In another report, poly(amidoamine) dendrimer (PAMAM) served as a template for the formation of Pt NCs by reducing H<sub>2</sub>PtCl<sub>6</sub> with NaBH<sub>4</sub> and the reaction lasted for two weeks.<sup>4</sup> Kim's group synthesized Pt NCs deposited on DNA-graphene oxide composite and the process required several days to complete.<sup>9</sup> The phosphonate-functionalized Pt NCs were created at the oil-bath temperature of 120 °C after 6 hr and their application in hydrogen peroxide sensing has been explored.<sup>10</sup> These methods either involve long reaction time,<sup>4,8-9</sup> or relatively harsh experimental conditions.<sup>10</sup>

Hypochlorite ion is an important reactive oxygen species, serving as an essential antibacterial agent to life. Overproduction of hypochlorite can lead to a variety of diseases, such as atherosclerosis, arthritis, and cancers.<sup>11-14</sup> Hypochlorite ion is also

used for drinking water disinfecting and household bleaching.<sup>15</sup> Therefore, sensitive and selective detection of hypochlorite has been recently focused.<sup>11-12, 16-17</sup> For example, organic fluorescent probes have been used for hypochlorite sensing.<sup>11-12</sup> However, the organic dyes are not bright or photostable enough and their synthesis is time-consuming.<sup>18-19</sup> CdSe-ZnS quantum dots (QDs) also served as a fluorescent probe for hypochlorite assay.<sup>16</sup> The drawback of these QDs is that they are toxic and their surface modifications are rather complicated.

In this study, highly fluorescent BSA-templated Pt NCs have been facilely fabricated where BSA serves as a scaffold and NaBH<sub>4</sub> as a reductant. The synthesis of the Pt NCs requires less time (1 hr) and does not involve harsh experimental conditions (under room temperature). Furthermore, the Pt NCs stabilized by BSA exhibits good water-solubility and stability. Without any surface functionalization, the BSA-stabilized Pt NCs act as an efficient fluorescent probe for hypochlorite sensing.

## 2. Experimental

### 2.1. Reagents and apparatus

Bovine serum albumin (BSA), chloroplatinic acid hexahydrate (H<sub>2</sub>PtCl<sub>6</sub>·6H<sub>2</sub>O), sodium hypochlorite, and hydrogen peroxide were acquired from Sinopharm Chemical Reagent Co. Ltd. (Shanghai, China). Sodium borohydride (NaBH<sub>4</sub>), sodium sulfide, the reduced form of glutathione (GSH) and cysteine were purchased from Sigma-Aldrich. Other reagents were all of analytical grade and used without further purification.

TEM measurement was carried out on a JEOL JEM-2100 transmission electron microscope (Tokyo, Japan). The oxidation state of the Pt NCs was characterized by XPS (K-Alpha 1063, Thermo Fisher Scientific). UV-vis absorption spectra and fluorescence spectra were recorded on a UV-vis spectrophotometer (Shimadzu, UV-2450) and a fluorescence spectrophotometer (Hitachi, F-4600), respectively. Dynamic light scattering (DLS) and zeta potential measurements were carried out on a Malvern Zetasizer Nano ZS. The circular dichroism (CD) spectra were recorded on a Jasco 815 spectropolarimeter. The composition of the Pt NCs was determined by inductively coupled plasma-atomic emission spectroscopy (ICP-AES) (PS-6, Baird, USA).

## 2.2. Formation and characterization of Pt NCs

The typical synthesis procedures involved the premixing of BSA ( $43 \text{ mg mL}^{-1}$ ),  $\text{H}_2\text{PtCl}_6$  (8.2 mM), and NaOH (86 mM) under vigorous shaking, followed by addition of  $\text{NaBH}_4$  (8.2 mM). After reaction for 1 h, the Pt NCs were produced and then purified by dialysis (membrane MWCO = 500 Da) for three times (0.5 h for each time). The dialysis was used to remove excess amounts of small molecules, such as  $\text{H}_2\text{PtCl}_6$ , NaOH, and  $\text{NaBH}_4$ .

The BSA-stabilized Pt NCs were subject to DLS, zeta potential, CD, and ICP-AES measurements.

## 2.3. Detection of hypochlorite

The 10-fold diluted Pt NCs were mixed with various concentrations of sodium hypochlorite in aqueous solutions, and the fluorescence of the mixture was measured.

### 3. Results and discussion

#### 3.1. Spectral properties of Pt NCs

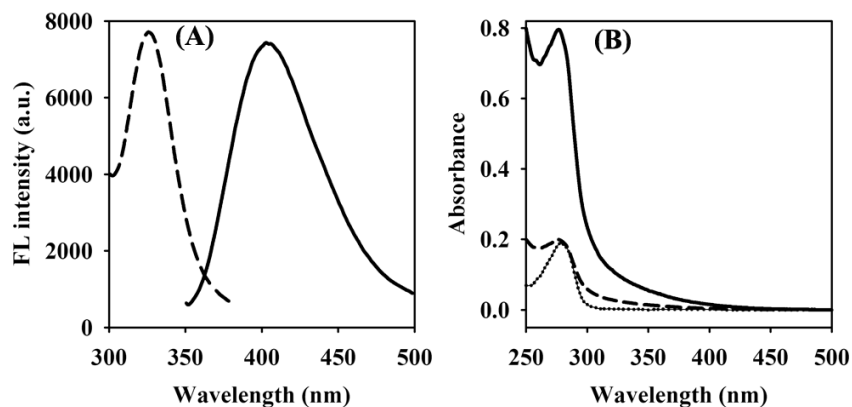


**Figure 1.** (A) Excitation (dashed curve) and emission (solid curve) spectra of Pt NCs (4-fold dilution). (B) UV-vis absorption spectra of BSA-templated Pt NCs in the absence (solid curve) and presence (dashed curve) of hypochlorite. The absorption spectrum of BSA was also displayed (dashed-dotted curve).

It is well known that BSA monomer contains 35 cysteine, 5 methionine and 2 tryptophan residues with a molecular weight of ca. 66 kDa and an isoelectric point of 4.7.<sup>2-3, 20</sup> The functional residues and the unique spatial structure of serum albumin enable the formation of various metal nanoclusters, such as gold,<sup>3</sup> silver,<sup>2</sup> and copper.<sup>1</sup> Typically, BSA serves as stabilizers and reductants in the formation of these NCs.<sup>1, 3</sup> The synthesis of Cu and Au NCs via sequestration and reduction of Cu and Au precursors by BSA has been demonstrated.<sup>1, 3</sup> However, under the similar experimental conditions, no fluorescent Pt NCs were produced when BSA was used to reduce  $\text{H}_2\text{PtCl}_6$ . As reported previously, the synthesis of Pt NCs is time-consuming



and involves relatively harsh experimental conditions.<sup>4, 8-9</sup> To circumvent these problems, one-pot synthesis of highly fluorescent Pt NCs was performed under the ambient conditions using NaBH<sub>4</sub> as a reductant and BSA as a scaffold. The excitation/emission spectra of the Pt NCs were displayed in Figure 1A. Strong fluorescence emission of the nanoclusters was attained at 404 nm upon excitation at 330 nm. However, under the same experimental conditions, BSA or the mixture of BSA and H<sub>2</sub>PtCl<sub>6</sub> did not fluoresce at 404 nm. It has been reported that BSA possesses weak intrinsic fluorescence at ca. 330 nm, which has been ascribed to the two tryptophan residues.<sup>20</sup> On the other hand, the UV-vis absorption in the region of 300–400 nm (solid curve in Figure 1B) indicates the formation of BSA-templated Pt NCs. While no absorption of BSA was observed in the same region except the characteristic peak at 270 nm (dashed-dotted curve).

The use of BSA as the capping agent favors the formation of the fluorescent Pt NCs. No fluorescence was obtained in the absence of BSA. However, the fluorescence of the Pt NCs increases with the BSA concentration and plateaus beyond 43 mg mL<sup>-1</sup>. Thus, the concentration of BSA was fixed at 43 mg mL<sup>-1</sup>. Without NaOH, very weak fluorescence was obtained, indicating that the alkali medium favors the formation of the highly fluorescent Pt NCs. Other NCs, such as BSA-stabilized Au NCs, were also created in the alkali medium.<sup>3</sup> The appropriate NaOH concentration for higher fluorescence is ca. 86 mM. Furthermore, the use of the strong reducing agent NaBH<sub>4</sub> is responsible for the increased reaction speed. Our method thus provides a good alternative for facile and efficient synthesis of Pt NCs.

### 3.2. Characterizations of Pt NCs

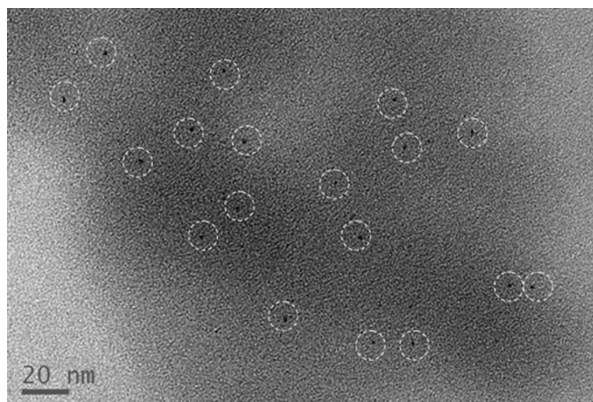


**Figure 2.** TEM image of the Pt NCs. For clarity, the Pt NCs were marked with circles.

As indicated in Figure 2, the Pt NCs possess uniform morphology with sub-nanometer sizes. Due to the extremely small size of the nanoclusters, the image has relatively low contrast. The difficulty in obtaining high-resolution images was ascribed to the decomposition of the Pt NCs upon high-energy electron irradiation.

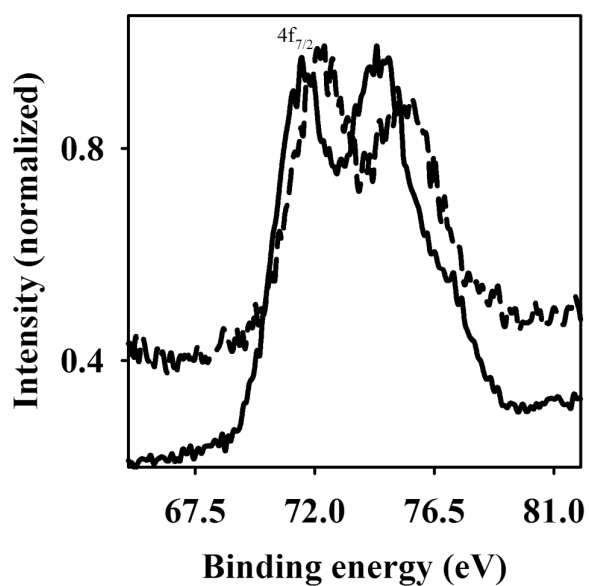


**Figure 3.** (A) Normalized Pt 4f XPS spectra of the Pt NCs in the absence (solid curve) and presence (long-dash curve) of hypochlorite.

The analysis of the oxidation states of the Pt NCs was performed by X-ray photoelectron spectroscopy (XPS) (Figure 3). The dried Pt NCs displayed a Pt 4f<sub>7/2</sub> peak at 71.5 eV, which is indicative of the reduced platinum Pt(0).<sup>8, 21</sup> The S and Pt levels in the BSA-capped Ag NCs were determined to be 438 and 1, 344 mg L<sup>-1</sup> by ICP-AES, respectively. Because one BSA molecule contains 40 S atoms (35 cysteine and 5 methionine residues),<sup>2</sup> the composition of the Pt NCs was estimated to be ca. Pt<sub>20</sub>/BSA.

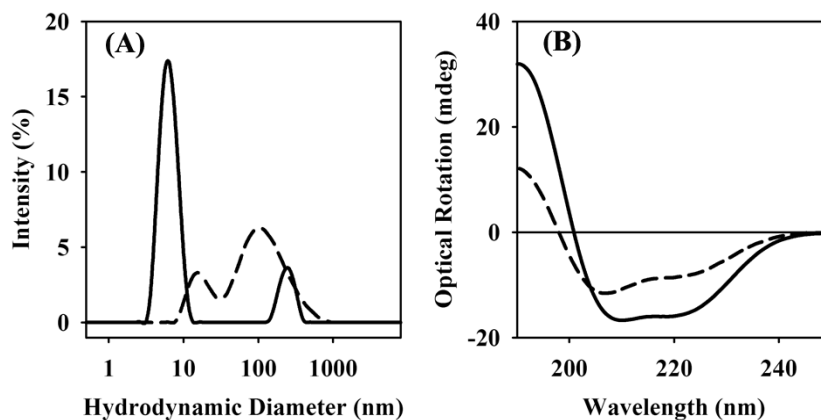


**Figure 4.** (A) DLS spectra of BSA (solid curve, 10-fold dilution) and BSA-stabilized Pt NCs (long-dashed curve, 10-fold dilution). (B) CD spectra of BSA (solid curve, 400-fold dilution) and BSA-stabilized Pt NCs (long-dashed curve, 400-fold dilution). BSA, which was premixed with NaOH and then NaBH<sub>4</sub>, followed by purification by dialysis, was used as a control.

The Pt NCs exerted a profound influence on the hydrodynamic diameter and secondary structure of the template BSA. As depicted by the solid curve in Figure 4A, BSA existed in two forms, with hydrodynamic diameters centered at 6.5 and 250 nm. The formation of Pt NCs inside the BSA molecules increased the hydrodynamic diameter of BSA from 6.5 nm to 13.5 nm (long-dashed curve in Figure 4A), suggesting the swelling of the protein.<sup>1</sup> Furthermore, the increased percentage of the form of BSA with hydrodynamic diameter of 250 nm (Figure 4A) might indicate the aggregation of the protein.<sup>1</sup> The zeta potential of the Pt NCs in aqueous solutions was determined to be  $-25 \pm 3.0$  mV, which might be ascribed to the encapsulation of the Pt NCs by the negatively charged BSA molecules. The BSA molecules endow the Pt NCs with good water-solubility and stability. We found that the Pt NCs were stable for at least a week when stored in the dark.

We also performed CD measurements to reveal the conformational behavior of BSA before and after the formation of Pt NCs. As shown by the solid curve in Figure 4B, BSA displayed CD features with negative absorption bands at 208 and 222 nm, which corresponds to the secondary structure of the protein.<sup>1, 22</sup> However, after the formation of Pt NCs, the shift of the 208-nm peak to 204 nm (long-dashed curve in Figure 4B) reveals a decrease of  $\alpha$ -helical content and an increase of  $\beta$ -structural element.<sup>1</sup>

### 3.3. Detection of hypochlorite

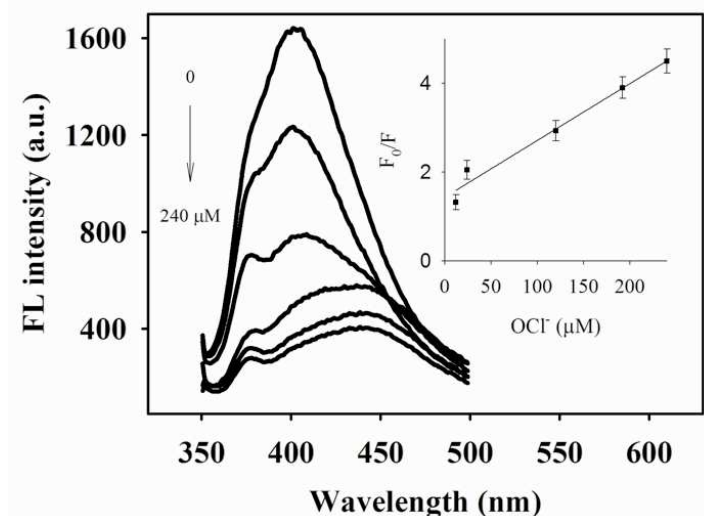


**Figure 5.** Fluorescence responses of Pt NCs toward hypochlorite with concentrations of 0, 12, 24, 120, 192, and 240  $\mu\text{M}$ . Inset: Plot of  $F_0/F$  versus hypochlorite concentration ranging from 12 to 240  $\mu\text{M}$ . Error bars were derived from three replicate measurements.

Although the Pt NCs or nanoparticles have been widely used in sensing applications relying on their catalytic activities,<sup>23-24</sup> few reports on the use of the Pt NCs as the fluorescent probe for chemical sensing have been documented. The feasibility of the method for the detection of hypochlorite has been demonstrated. In the presence of hypochlorite, the fluorescence of the Pt NCs was quenched remarkably (Figure 5). The  $F_0/F$  ( $F_0$  and  $F$  represent the fluorescence intensities in the absence and presence of hypochlorite, respectively) is linearly correlated with the concentration of hypochlorite ranging from 12 to 240  $\mu\text{M}$  (inset of Figure 5). The linear regression equation of  $F_0/F = 0.013 C [\mu\text{M}] + 1.44$  was obtained ( $R^2 = 0.98$ ). As shown in Figure 6, certain thiol compounds,  $S^{2-}$ , common oxidants, and heavy metal

ions exerted little influence on the fluorescence of Pt NCs. However, the interferents, such as  $\text{H}_2\text{O}_2$ , thiols, and  $\text{S}^{2-}$  were capable of quenching the emission of Au NCs,<sup>25</sup> Ag/Au NCs,<sup>26</sup> and Ag/Au NCs.<sup>27</sup>

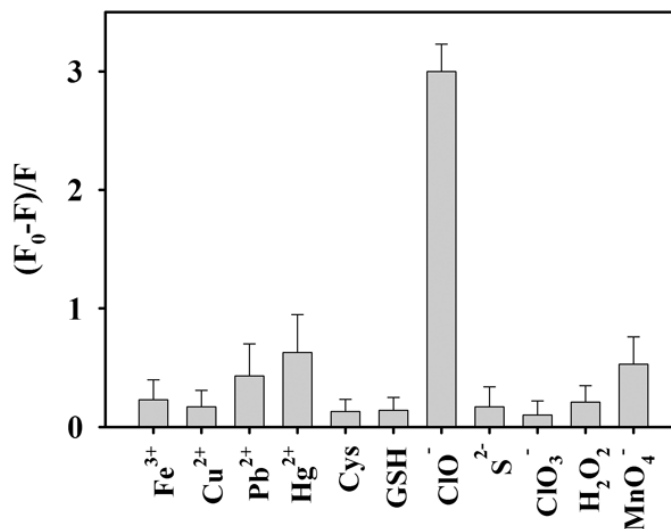


**Figure 6.** Selectivity toward hypochlorite assay in which 10-fold diluted Pt NCs were used. The concentrations of hypochlorite and the interferences were all 120  $\mu\text{M}$ . Error bars were derived from three replicate measurements.

The mechanism underlying the fluorescence quenching was further explored by XPS and UV-vis absorption spectroscopy. Upon incorporation of hypochlorite, the Pt  $4f_{7/2}$  peak shifted from 71.5 to 72.3 eV (Figure 3), implying the oxidation of Pt NCs by hypochlorite.<sup>8</sup> The significantly decreased UV-vis absorption of Pt NCs in the region of 300–400 nm and at 270 nm in the presence of hypochlorite (dashed curve in Figure 1B) again supports the oxidation of Pt NCs. It is well-known that hypochlorite possesses higher oxidation ability than  $\text{H}_2\text{O}_2$ , thus the Pt NCs are stable toward  $\text{H}_2\text{O}_2$ . The higher stability of the nanoclusters is originated from the strong affinity between

cysteine residues of BSA and noble metal ions. As a result, interferents, such as certain thiol compounds,  $S^{2-}$ , common oxidants, and heavy metal ions exerted negligible influence on the fluorescence of Pt NCs. The proof-of-concept experiment demonstrates the potential of Pt NCs for selective detection of hypochlorite.

#### 4. Conclusions

A rapid and facile method for the fabrication of highly fluorescent BSA-templated Pt NCs has been developed. The formation of Pt NCs inside the BSA molecules has a great influence on the hydrodynamic diameter and secondary structure of the template BSA. The composition of the Pt NCs was determined to be ca. Pt<sub>20</sub>/BSA. The Pt NCs serve as an efficient probe for the detection of hypochlorite. The sensing mechanism involves the oxidation of Pt NCs by hypochlorite. The assay of hypochlorite is highly selective since the interferents investigated exerted negligible influence on the fluorescence of Pt NCs.

#### Acknowledgments

Partial support of this work by the National Natural Science Foundation of China (No. 21375150, 21175156) and the Specialized Research Fund for the Doctoral Program of Higher Education (No. 20100162110018) is gratefully acknowledged.

## References

1. N. Goswami, A. Giri, M. S. Bootharaju, P. L. Xavier, T. Pradeep and S. K. Pal, *Anal. Chem.*, 2011, 83, 9676.
2. C. Guo and J. Irudayaraj, *Anal. Chem.*, 2011, 83, 2883.
3. J. Xie, Y. Zheng and J. Y. Ying, *J. Am. Chem. Soc.*, 2009, 131, 888.
4. S. I. Tanaka, J. Miyazaki, D. K. Tiwari, T. Jin and Y. Inouye, *Angew. Chem. Int. Ed.*, 2011, 50, 431.
5. H. Qian, M. Zhu, Z. Wu and R. Jin, *Acc. Chem. Res.*, 2012, 45, 1470.
6. Z. Wu and R. Jin, *Nano Lett.*, 2010, 10, 2568.
7. H.-C. Yeh, J. Sharma, I.-M. Shih, D. M. Vu, J. S. Martinez and J. H. Werner, *J. Am. Chem. Soc.*, 2012, 134, 11550.
8. X. Le Guevel, V. Trouillet, C. Spies, G. Jung and M. Schneider, *J. Phys. Chem. C*, 2012, 116, 6047.
9. J. N. Tiwari, K. Nath, S. Kumar, R. N. Tiwari, K. C. Kemp, N. H. Le, D. H. Youn, J. S. Lee and K. S. Kim, *Nat. Commun.*, 2013, 4, 2221.
10. J. Xu, X. Wu, G. Fu, X. Liu, Y. Chen, Y. Zhou, Y. Tang and T. Lu, *Electrochim. Acta*, 2012, 80, 233.
11. F. Wei, Y. Lu, S. He, L. Zhao and X. Zeng, *Anal. Method.*, 2012, 4, 616.
12. X. Chen, X. Wang, S. Wang, W. Shi, K. Wang and H. Ma, *Chem. Eur. J.*, 2008, 14, 4719.
13. D. I. Pattison and M. J. Davies, *Chem. Res. Toxic.*, 2001, 14, 1453.
14. A. Kettle and C. Winterbourn, *Redox Rep.*, 1997, 3, 3.
15. F. Wei, Y. Lu, S. He, L. Zhao and X. Zeng, *J. Fluoresc.*, 2012, 22, 1257.
16. Y. Yan, S. Wang, Z. Liu, H. Wang and D. Huang, *Anal. Chem.*, 2010, 82, 9775.
17. D. Zhang, *Spectrochim. Acta A*, 2010, 77, 397.
18. T. Vosch, Y. Antoku, J.-C. Hsiang, C. I. Richards, J. I. Gonzalez and R. M. Dickson, *Proc. Nat. Acad. Sci.*, 2007, 104, 12616.
19. C. I. Richards, S. Choi, J.-C. Hsiang, Y. Antoku, T. Vosch, A. Bongiorno, Y.-L. Tzeng and R. M. Dickson, *J. Am. Chem. Soc.*, 2008, 130, 5038.
20. N. Tayeh, T. Rungassamy and J. R. Albani, *J. Pharm. Biomed. Anal.*, 2009, 50, 107.
21. A. Arico, A. Shukla, H. Kim, S. Park, M. Min and V. Antonucci, *Appl. Sur. Sci.*, 2001, 172, 33.
22. N. S. Quiming, R. B. Vergel, M. G. Nicolas and J. A. Villanueva, *J. Health Sci.*, 2005, 51, 8.
23. W. Liu, H. Wu, B. Li, C. Dong, M. M. F. Choi and S. Shuang, *Anal. Method.*, 2013, 5, 5154.
24. E. Spain, H. McArdle, T. E. Keyes and R. J. Forster, *Analyst*, 2013, 138, 4340.
25. X. Xia, Y. Long and J. Wang, *Anal. chim. acta*, 2013, 772, 81.
26. Y.-T. Su, G.-Y. Lan, W.-Y. Chen and H.-T. Chang, *Anal. Chem.*, 2010, 82, 8566.
27. W.-Y. Chen, G.-Y. Lan and H.-T. Chang, *Anal. Chem.*, 2011, 83, 9450.